Effect of Thermo-mechanical Treatment on Microstructure and Mechanical Properties of Two-phase TiNbO Alloy

Wang Junshuai* [1], Ma Chaoli[1], Xiao Wenlong[1]

[1] *School of Materials Science and Engineering, Beihang University, Beijing, China*

Abstract

We designed the composition of alloy with Ti-8Nb-0.5O (at. %) and fabricated in high vacuum arc-melting furnace. This work was focused on the effect of thermo-mechanical treatment on microstructure and mechanical properties. Transmission Electron Microscope (TEM), Scanning Electron Microscope (SEM), X-ray Diffraction analysis (XRD), Micro Vickers Hardness Tests and Tensile Tests were utilized to characterize the alloys. The annealing temperature has a significant effect on the microstructure and mechanical properties of TiNbO alloy. When the alloy was annealed at 300℃, 400℃ or at hot-rolled state, there were just α and β phases in the alloy. When the alloy was annealed at 500℃, 600℃, the alloy recrystallized and harmful ω phase appeared, which increased the modulus and strength of the alloy greatly. When the alloy is annealed at 700℃, the alloy recrystallized completely without ω phase. When we accelerated the cooling rate after annealed, the martensitic transformation appeared, which restrained the appearance of ω phase and reduced the modulus.

1.Introduction

Recently, Titanium alloys have attracted more and more attention and have been widely used in various medical implant materials due to their excellent mechanical, corrosion resistance and enhanced biocompatibility，especially low Young's modulus[1-3]. The modulus is particularly important for implant materials which may cause stress shielding effect, a phenomenon where reabsorption of natural bone and implant loosening arises because of the mismatch in elastic modulus between natural bone and hard tissue implant[4]. However, widely used biomedical titanium-based materials (such as pure Ti, Ti-6Al-4V) still have higher elastic modulus compared with human bones (10-30 GPa) [5]. Besides, they are found to be unsuitable for biomedical applications owing to the toxic effect of both Al and V and may cause long-term health problems[6]. In general, a new generation of low modulus β titanium alloys, which are free of V and Al, has been made with β-stabilizing and biocompatible elements such as Nb, Ta and Zr[7].

It was pointed out that that Ti-Nb alloys show low Young's modulus and have a strong dependence of E on the chemical composition[8]. It is interesting to note that Young's modulus for Ti-Nb alloys quenched from the β phase region exhibits two minima at 8 at. % and 24 at. % Nb. However, binary Ti-Nb alloys exhibit lower strength due to the presence of stress-induced martensite, which restrict their application range. The strength of β-Ti alloys usually need to be improved by solution strengthening of alloying elements (N and O), or precipitation strengthening by α or ω phases.

The addition of O to β Ti alloys has been found to some special effects. Oxygen, which is regarded as an interstitial element, has a significant solid solution strengthening effect and keeps its Young's modulus relatively low [9-11]. It was reported by Kim [12] that the fracture stress of solution treated specimen increased with increasing oxygen content. Nii et al. [13] has found that the addition of 0.3 at.% oxygen in Ti-26Nb alloy resulted in the formation of nanosized martensite and suppressed long-range martensitic transformation upon cooling, which increased the stress required to induce martensitic transformation. It is reported that thermo-mechanical treatment could get the precipitation of nanosized α and ω phase in the matrix β phase and refine grain [14-17]. The critical stress for slip increases with increase in amount of α and/or ω phase precipitates in general [15, 18-20].

In this present study, Ti-8Nb-0.5O (at. %) alloy was designed in order to develop biomedical alloys with low Young's modulus and high strength. On the basis of the combined results from X-ray diffraction, transmission electron microscopy and tensile test, the influence of annealing temperature on microstructure and mechanical properties was discussed.

2.Material and Experimental

The alloy was fabricated in high vacuum arc-melting furnace. TiO2 powder (99.9%) wrapped in pure Ti foil was also melted with Ti (99.9%) and Nb (99.99%). The oxygen content was controlled by the amount of TiO2 powder. In order to guarantee the sample uniformity, the ingot was melted repeatedly for 6 times. Then the ingot was subjected to a homogenization at 1000℃ for 7.2ks in an Ar gas atmosphere, followed by water quenching. Then the ingot was hot rolled at 600℃ to thickness reductions of up to 85% so as to have the final thickness of 1.5mm. The rolled specimens were annealed at the temperature rage 300-700 ℃ for 3.6 ks in Ar atmosphere, followed by air cooling. And some rolled specimens were annealed at 600 ℃, followed by water quenching, to analyze the effect of cooling rate.

Specimens for tensile test with a gage length of 18mm were spark cut along the rolling direction. Tensile tests were conducted on an Instron 8801 machine at a strain rate of 0.5 mm/min. The micro-hardness of alloys was tested by Vickers hardness tester at a load of 300gf for 15s. The phase constitutions were determined by X-ray diffraction (XRD) with Cu Kα radiation at an accelerating voltage of 40 kV and a current of 250 mA. The Microstructures were identified by optical microscopy (OM) and

transmission electron microscope (TEM). TEM specimens were prepared by a conventional twin-jet electro-polishing technique with a solution of hydrofluoric acid/sulfuric acid/methanol at 2:5:93 by volume under 30V at about 233 K.

3.Results and discussion

Optical micrographs of the specimens hot rolled and annealed at different temperature are presented in Fig. 1. It is clear that microstructure can be divided into two categories. The black banded structure can be observed in specimens hot rolled and annealed at 300 and 400 ℃. The deformation bands introduced in the process of rolling still exist at low temperature annealing. And the structure shows a darker color relative to the matrix after corrosion. When the annealing temperature higher than 500℃, the microstructure of specimens are formed by very fine globular α phase in β matrix without obvious β grain boundary and deformation bands. This is because the annealing temperature exceeds the recrystallization temperature of the alloy, and a large number of broken crystal grains caused by the rolling process are recrystallized to form very fine dispersed grains.

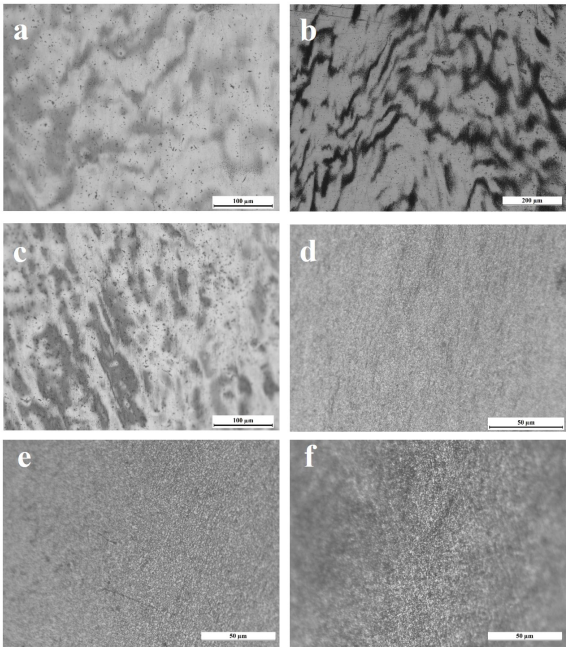

Fig.1 OM images of the specimens. Hot rolled(a), annealed at 300℃(b), 400℃(c), 500℃(d), 600℃(e), 700℃(f)

In order to identify the constituent phases of each annealed specimens X-ray diffraction measurement was carried out. Figure 2 shows X- ray diffraction profiles of the specimens hot rolled and annealed at different temperature. It is clear from the XRD profiles that the specimens in all states contain both α and β phases, which are consistent with the results of the optical micrographs. This also means that the α/β transus temperature of Ti-8Nb-0.5O is below 700 ℃. In comparison with the annealed specimens, the diffraction peak broadening after the hot rolling suggests a significant effect due to grain refinement. It's worth noting that the ω peaks appear in the specimens annealed at 600℃. This indicates that ω phase was precipitated in the cooling process after annealing at 600℃.

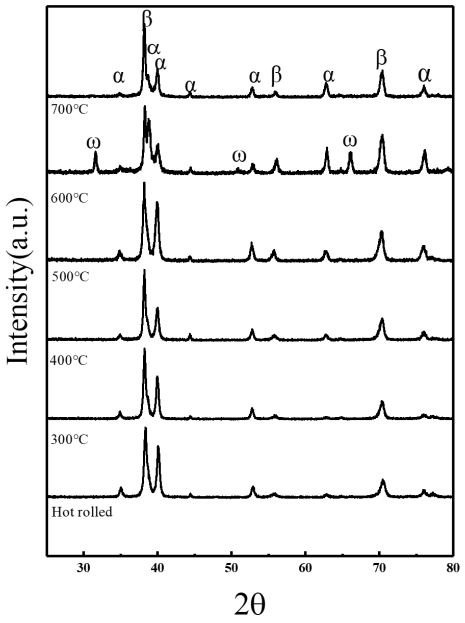

Fig.2 XRD of specimens in different heat treatment

Figure 3 shows bright field images and the corresponding selected area diffraction patterns (SADP) in the specimens hot rolled and annealed at different temperature. It can be seen that there are many black areas (indicated by the arrow) in the hot rolled and the annealed at 300 ° C and 400 ° C specimens, which are caused by a large number of dislocations. The diffraction spots are dense and ring-shaped, indicating that after a large number of deformations, the grains are significantly refined. Besides, the diffraction ring analysis shows that both specimens contain α+β two phases. And the results are also consistent with the OM and XRD. In the specimens annealed at 500 and 600 ℃， it can be seen that the alloy has undergone significant recrystallization with grain size about 1μm. The [113]β SAD pattern of 600 ℃ annealed specimen clearly shows the existence of ω phase. Apart from the primary {110}β and {002β reflections of the bcc β matrix, distinct secondary intensity maxima and reciprocal lattice streaking are visible at the 1/3 and 2/3 {112}β position, which result from the diffraction of the ω lattice. The orientation relationship of the β matrix and the ω phase is {111}β‖{0001}ω and <110>β‖<11-20>ω， as usually reported for thermally induced β to ω transformation[21]. However, specimens annealed at 700 ℃ completely recrystallized without ω phase. This is likely due to the fact that O atoms diffuse into the β matrix during annealed at higher temperatures. It is generally understood that the ω phase is formed owing to the collapse of neighboring {111}β planes to an intermediate position. In this case, the suppression of the ω-phase formation due to oxygen addition is likely to occur, because oxygen interferes with atomic displacement during the diffusion-less transformation from the β phase to the ω phase[22].

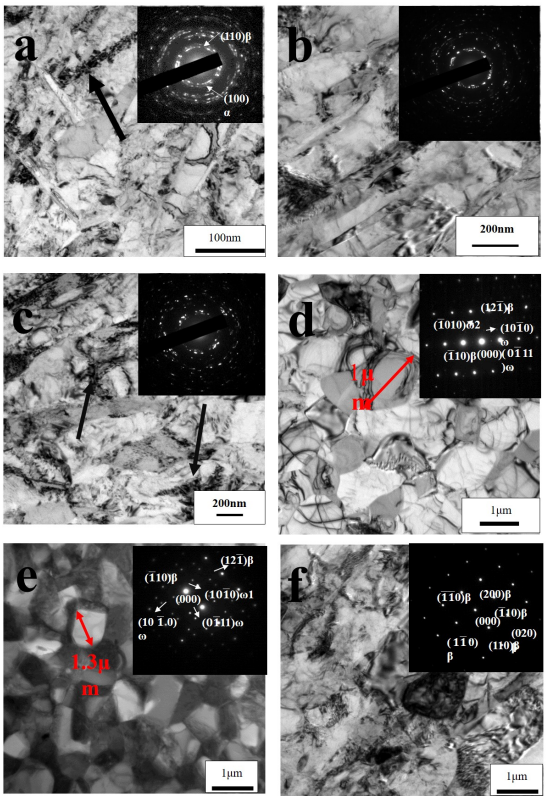

Fig.3 TEM images and SADP of specimens . Hot rolled(a), annealed at 300℃(b), 400℃(c), 500℃(d), 600℃(e), 700℃(f)

The mechanical properties of alloys were determined by uniaxial tensile testing. The corresponding stress-strain curves are plotted in Fig. 4, and the mechanical properties are given in Table 1. It can be seen from the figure that all of the specimens exhibit a certain stress softening after yielding, and the stress gradually decreases as the strain increases. As the annealing temperature increases, the strength of the alloy shows a downward trend. However, the annealed specimens at 600 ° C exhibit an abnormally high tensile strength of up to 880 MPa. The elongation of each alloy also generally shows a tendency to increase with increasing annealing temperature, but the specimens annealed at 500 ° C and 600 ° C exhibit relatively low elongation. While the specimens annealed at 700 ° C have highest elongation. For the elastic modulus and hardness, the 600 °C annealed specimen shows the highest value, and the other specimens show little change. The performance of the mechanical properties of these alloys is strongly related to their microstructure. The reason why the 600 ° C annealing samples have high strength, high modulus, high hardness and low elongation is the large amount of fine dispersed ω phase contained therein. While the ω phase is a hard and brittle phase, the ω phases greatly strengthen the alloy, which improves the strength and hardness of the alloy. But at the same time the ω phases greatly increase the modulus of the alloy and reduce the elongation of the alloy. Although the 500 °C annealing specimens also contain ω phase, the content is less than 600℃ annealing specimens, which is also consistent with the absence of the ω phase detected in the XRD. Therefore, the strength, modulus, and hardness change are not as large as the 600 °C annealing specimens. However, the partial decrease in the low elongation of the 500 ° C annealing specimens is also related to the small amount of ω phase contained therein. In addition, under low temperature annealing, the specimens didn't completely recrystallize, and some of the remaining dislocations also contribute to the strength. On the other hand, it can be observed that the elongation of the 700 ° C annealing sample is large. This is explained by the fact that both the α and β phases are continuously coarsened, so that high plasticity is produced.

Table 1 Mechanical properties of specimens

Specimens	E (GPa)	$\sigma_{0.2}$ (MPa)	σ_b (MPa)	δ (%)	HV
Hot rolled	65	637	852	27	244±8
300℃	76	688	864	28	244±10
400℃	55	681	813	31	250±8
500℃	71	660	794	26	230±5
600℃	101	825	881	17	292±15
700℃	80	641	746	37	234±6

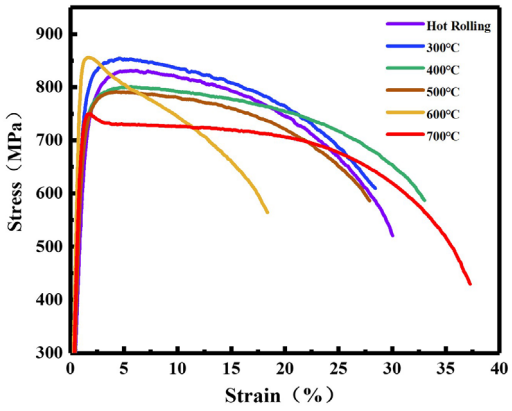

Fig.4 Strain-stress curves of specimens

It has been reported in the literature that increasing the cooling rate can suppress the precipitation of ω phase[23]. In order to eliminate the effect of harmful ω phase, some rolled specimens were annealed at 600 ℃, followed by water quenching (WQ). As shown in figure 5, we don't find the diffraction peaks of the α and the ω phase in water quenching specimens. However, there are plenty martensite α" phase. The martensite transformation is a non-diffusion phase transition. When the β-stabilizing element in the alloy is lee and the cooling rate is faster, the β phase forms orthorhombic α" phase directly without α and ω phases. Besides, the WQ specimens have lower Young's modulus and strength compared and higher elongation compared with AQ specimens. The change is related to the disappearance of ω phase and the appearance of α" phase.

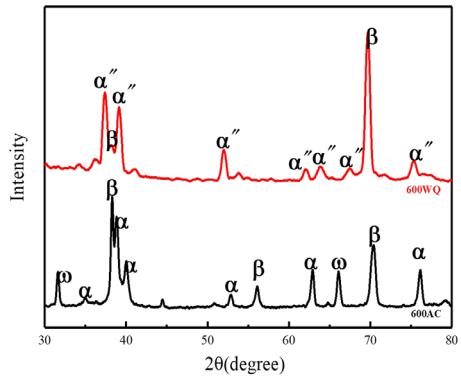

Fig.5 XRD of specimens in different cooling rate

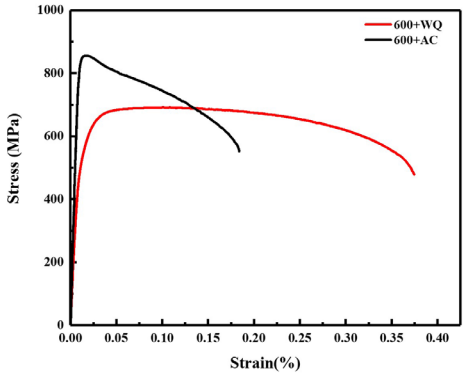

Fig.6 Strain-stress curves of specimens in different cooling rate

4.Conclusion

In this study, thermo-mechanical treatment of Ti-8Nb-0.5O alloy was carried out, and the effects of different annealing temperatures on the microstructure and mechanical properties of the alloy were analyzed.

(1) After annealing at different temperatures, the alloys contain α and β phases. Annealing at lower temperatures (≤400 °C), the alloy mainly undergoes dislocation recovery. Annealing at a higher temperature, the alloy is recrystallized, and a fine grain structure having a grain size of about 1 μm can be obtained.

(2) With the increase of annealing temperature, the strength of the alloy shows a downward trend, and the plasticity shows an upward trendency.

(3) After annealing at 600 °C, a large amount of ω phase is precipitated in the alloy, which leads to the alloy exhibiting the highest strength and Young's modulus, and the lowest elongation. Increasing the cooling rate can suppress the precipitation of the ω phase.

5.Acknowledgements

The authors are grateful to the financial support by International Science and Technology Cooperation Program of China (2015DFA51430), National Natural Science Foundation of China (NSFC, No. 51671012, 51671007 and 51401010) and Aeronautical Science Foundation of China (2015ZF51069) and to carry out this work.

6.References

[1] M. Geetha, A. K. Singh, R. Asokamani and A. K. Gogia, Progress in Materials Science. 54 (2009) 397-425.

[2] M. T. Mohammed, Z. A. Khan and A. N. Siddiquee, 8 (2014) 7.

[3] M. Niinomi, Materials Science and Engineering: A. 243 (1998) 231-236.

[4] A. Meunier, P. Christel, L. Sedel, J. Witvoet and D. Blanquaert, International Orthopaedics. 14 (1990) 67-73.

[5] Y. Li, C. Yang, H. Zhao, S. Qu, X. Li and Y. Li, Materials (Basel). 7 (2014) 1709-1800.

[6] M. Abdel-Hady Gepreel and M. Niinomi, J Mech Behav Biomed Mater. 20 (2013) 407-15.

[7] M. Niinomi, J Mech Behav Biomed Mater. 1 (2008) 30-42.

[8] S. Hanada, T. Ozaki, E. Takahashi, S. Watanabe, K. Yoshimi and T. Abumiya, Materials Science Forum. 426-432 (2003) 3103-3108.

[9] M. Yan, W. Xu, M. S. Dargusch, H. P. Tang, M. Brandt and M. Qian, Powder Metallurgy. 57 (2014) 251-257.

[10] Q. Li, D. Ma, J. Li, M. Niinomi, M. Nakai, Y. Koizumi, D. Wei, T. Kakeshita, T. Nakano, A. Chiba, K. Zhou and D. Pan, MATERIALS TRANSACTIONS. 59 (2018) 858-860.

[11] J. I. Qazi, V. Tsakiris, B. Marquardt and H. J. Rack, Journal of ASTM International. 2 (2005).

[12] J. I. Kim, H. Y. Kim, H. Hosoda and S. Miyazaki, Materials transactions. 46 (2005) 852-857.

[13] Y. Nii, T.-h. Arima, H. Y. Kim and S. Miyazaki, Physical Review B. 82 (2010).

[14] Q. Meng, S. Guo, Q. Liu, L. Hu and X. Zhao, Progress in Natural Science: Materials International. 24 (2014) 157-162.

[15] S. J. Li, Y. W. Zhang, B. B. Sun, Y. L. Hao and R. Yang, Materials Science and Engineering: A. 480 (2008) 101-108.

[16] L. L. Pavón, E. L. Cuellar, S. V. Hernandez, I. E. Moreno-Cortez, H. Y. Kim and S. Miyazaki, Journal of Alloys and Compounds. 782 (2019) 893-898.

[17] S. Guo, Q. Meng, G. Liao, L. Hu and X. Zhao, Progress in Natural Science: Materials International. 23 (2013) 174-182.

[18] Q. Meng, Q. Liu, S. Guo, Y. Zhu and X. Zhao, Progress in Natural Science: Materials International. 25 (2015) 229-235.

[19] A. Helth, S. Pilz, T. Kirsten, L. Giebeler, J. Freudenberger, M. Calin, J. Eckert and A. Gebert, J Mech Behav Biomed Mater. 65 (2017) 137-150.

[20] S. Ozan, J. Lin, Y. Li, Y. Zhang, K. Munir, H. Jiang and C. Wen, J Mech Behav Biomed Mater. 78 (2018) 224-234.

[21] S. K. Sikka, Y. K. Vohra and R. Chidambaram, Progress in Materials Science. 27 (1982) 245-310.

[22] M. Nakai, M. Niinomi, T. Akahori and H. Tsutsumi, Materials Science Forum. 654-656 (2010) 2134-2137.

[23] D. L. Moffat and D. C. Larbalestier, Metallurgical Transactions A. (1988).